Inorganic Chemistry

Article

pubs.acs.org/IC

# Luminescent Li-Based Metal–Organic Framework Tailored for the Selective Detection of Explosive Nitroaromatic Compounds: Direct Observation of Interaction Sites

Tae Kyung Kim,[†] Jae Hwa Lee,[†] Dohyun Moon,*[,‡] and Hoi Ri Moon*[,†]

[†]Interdisciplinary School of Green Energy and KIER-UNIST Advanced Center for Energy, Ulsan National Institute of Science and Technology (UNIST), UNIST-gil 50, Ulsan 689-798, Republic of Korea

[‡]Beamline Division, Pohang Accelerator Laboratory, San-31, Hyoja-Dong, Nam-Gu, Pohang, Kyungbuk 790-784, Korea

Supporting Information

**ABSTRACT:** A luminescent lithium metal–organic framework (MOF) is constructed from the solvothermal reaction of $Li^+$ and a well-designed organic ligand, bis(4-carboxyphenyl)-*N*-methylamine ($H_2$CPMA). A Li-based MOF can detect an explosive aromatic compound containing nitro groups as an explosophore, by showing a dramatic color change with concurrent luminescence quenching in the solid state. The detection sites are proven directly through single-crystal-to-single-crystal transformations, which show strong interactions between the aromatic rings of the electron-rich $CPMA^{2-}$ molecules and the electron-deficient nitrobenzene.

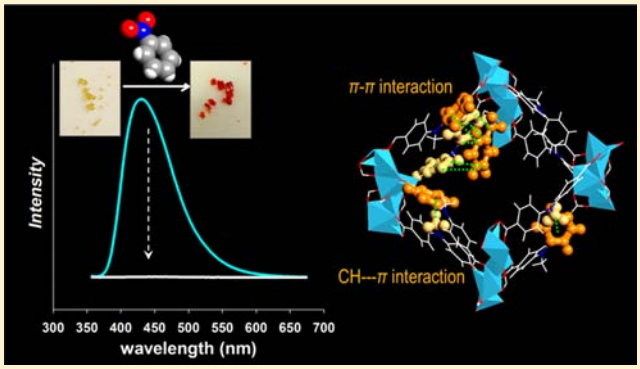


## INTRODUCTION

Metal–organic frameworks (MOFs) have received much attention because of their potential applications in gas storage,[1] catalysis,[2] molecular separation,[3] and sensing.[4−8] In order to live up to these expectation, various efforts have been made in the development of apposite materials such as the introduction of diverse metal ions with different coordination geometries and the design of functionalized organic ligands.

In particular, organic ligands as structure-directing building units provide two important features for MOFs: (1) added flexibility and diversity in the geometric structures of MOFs[9−11] and (2) alteration of the electronic structures and surface functionalities of MOFs.[12−14] Because the structure of a MOF is the decisive factor in these functionalities, various symmetry conformations, lengths and dimensions, and numbers of coordinating groups in the ligands have been adopted for the construction of functional MOFs.[9−11] In addition, functionalization of the framework ligand with strong electron-withdrawing and/or -donating groups enhances the surface interaction of MOFs toward specific analytes and generates luminescent properties in MOFs.[12−14] Recently, Cao et al. reported the effects of ligand functionalization on hydrogen storage in MOFs by spillover. An MOF constructed with the ligands possessing strongly electrophilic functional groups showed a remarkably enhanced hydrogen uptake because of thermodynamically favored hydrogenation.[13] Using *trans*-4,4′-stilbenedicarboxylic acid as an organic building block, the Allendorf group prepared Zn-MOF analogous to an isoreticular MOF, which possesses ligand-based luminescence in the solid state.[14]

Luminescent MOFs can be applied in the detection of hazardous substances, which is a very important aspect in terms of environmental and safety considerations. Several MOFs showed selective and fast detection of toxic aromatic compounds via a fluorescence quenching mechanism.[4−7] Most recently, a highly luminescent MOF, $[Zn_2(oba)_2(bpy)]$ [$H_2$oba = 4,4′-oxybis(benzoic acid); bpy = 4,4′-bipyridine], was found to exhibit unique selectivity for the detection of high explosives and other aromatics via a fluorescence quenching and enhancement mechanism.[5] In that report, the explanation of the quenching/enhancement mechanism relied on molecular-orbital and electronic band-structure calculations.

Herein, we report the synthesis of a well-defined ditopic organic ligand, $H_2$CPMA, for the potential provision of luminescence properties in MOFs, and the successful preparation of the luminescent three-dimensional Li-based MOF, $\{Li_3[Li(DMF)_2](CPMA)_2\}\cdot 4DMF\cdot H_2O$ [**1**; DMF = *N*,*N*′-dimethylformamide, $H_2$CPMA = bis(4-carboxyphenyl)-*N*-methylamine], by using the tailored $H_2$CPMA ligand and a $Li^+$ cation. The luminescent MOF was examined as a detector of toxic and explosive aromatic compounds containing nitro groups as an explosophore by changing its visible color as well as showing luminescence quenching in the solid state. Significantly, we provide direct evidence for alteration of the

**Received:** May 30, 2012
**Published:** December 27, 2012

   dx.doi.org/10.1021/ic3011458 | *Inorg. Chem.* 2013, 52, 589−595

electronic structure of **1** upon a representative nitroaromatic compound, nitrobenzene sensing by single-crystal-to-single-crystal transformation. The single-crystal X-ray diffraction (XRD) results for **1**⊃nitrobenzene clearly showed strong $\pi-\pi$ interactions between nitrobenzene and the benzene rings of $CPMA^{2-}$ in **1** and the inducement of CH$\cdots\pi$ interactions between neighboring $CPMA^{2-}$ ligands in the framework.

## EXPERIMENTAL SECTION

**Materials and Methods.** All chemicals and solvents used in the syntheses were of reagent grade and were used without further purification. Fourier transform (FT)-NMR spectra were measured by a Varian 600 MHz spectrometer. IR spectra were recorded with a ThermoFisher Scientific Nicolet 6700 FT-IR spectrophotometer. Elemental analyses were performed at the UNIST Central Research Facilities Center in Ulsan National Institute of Science and Technology (UNIST). UV/vis spectra were recorded with a Cary 5000 UV/vis spectrophotometer. Fluorescence spectra were measured with a Cary Eclipse fluorescence spectrometer. Thermogravimetric analysis (TGA) was performed under a $N_2$(g) atmosphere at a scan rate of 5 °C $min^{-1}$ using Q50 from TA Instruments. X-ray photoelectron spectroscopy (XPS) was performed using a Thermo Scientific K-Alpha XPS spectrometer.

**Synthesis of $H_2$CPMA.** $H_2$CPMA was prepared by modifying the methods reported in the previous study.[15] *N*-Methyldiphenylamine (6 mL, 33.6 mmol) was dissolved in chloroform (100 mL), to which a chloroform solution (70 mL) of dibromine (1.8 mL, 34.9 mmol) was slowly added at 0 °C. After stirring at 0 °C for 3 h, the solution was evaporated under reduced pressure, which resulted in a pale-yellowish oily residue. Methanol (MeOH) was added to the residue until white microcrystals of bis(4-bromophenyl)-*N*-methylamine were formed. The product was filtered, washed with MeOH, and dried briefly in air. Yield: 3.9 g (35%). $^1$H NMR (DMSO-$d_6$): $\delta$ 7.43 (d, 4H), 6.97 (d, 4H), 3.22 (s, 3H). Bis(4-bromophenyl)-*N*-methylamine (1.0 g, 2.9 mmol) was dissolved in freshly distilled tetrahydrofuran (40 mL) in an Ar(g) atmosphere, and *n*-butyllithium (1.6 M hexane, 12 mL, 19 mmol) was added to the solution at −78 °C. After the solution was stirred for 3 h, crushed dry ice was added, and a white precipitate immediately formed. The white precipitate suspended in the solution was kept at room temperature for 4 h, and acetic acid was added to the solution until the precipitate was completely dissolved. After the solution was filtered, the filtrate was concentrated and added to cold water. The resulting precipitate was filtered, washed with water, and dried under reduced pressure at ambient temperature. Yield: 0.62 g (79%). $^1$H NMR (DMSO-$d_6$): $\delta$ 7.86 (d, 4H), 7.15 (d, 4H), 3.31 (s, 3H). FT-IR (KBr pellet): $\nu_{O-C=O}$ 1673(s), 1593(s) $cm^{-1}$.

**Synthesis of $\{Li_3[Li(DMF)_2](CPMA)_2\}\cdot 4DMF\cdot H_2O$ [1; DMF = *N*,*N*′-Dimethylformamide, $H_2$CPMA = Bis(4-carboxyphenyl)-*N*-methylamine].** $H_2$CPMA (0.040 g, $1.5 \times 10^{-1}$ mmol) was dissolved in DMF (2 mL) and added to a DMF solution (3 mL) of $LiNO_3\cdot 6H_2O$ (0.021 g, $3.0 \times 10^{-1}$mmol). The mixture was placed in a Teflon vessel within the autoclave, heated, and kept at 150 °C for 12 h. The temperature was sequentially raised to 180 °C and kept for another 24 h. The solution was cooled to room temperature and kept until pale-yellow rodlike crystals resulted. The crystals were filtered off and washed briefly with DMF. Yield: 22%. FT-IR for **1** (Nujol mull): $\nu_{C=O(DMF)}$ 1678, $\nu_{O-C=O(carboxylate)}$ 1595, $\nu_{C=C(aromatic)}$ 1557 $cm^{-1}$. UV/vis (diffuse reflectance, $\lambda_{max}$): 339, 283 nm. Anal. Calcd for $Li_4C_{48}H_{66}O_{15}N_8$: C, 56.36; H, 6.50; N, 10.95. Found: C, 56.50; H, 6.08; N, 11.11.

**Detection of Nitrobenzene in 1.** $\{Li_3[Li(H_2O)_2]\text{-}(CPMA)_2\}\cdot 3$nitrobenzene$\cdot 2$DMF (**1**⊃nitrobenzene): Freshly prepared pale-yellow crystals of **1** (0.032 g, $3.13 \times 10^{-2}$mmol) were immersed in nitrobenzene for 8 days. The color of **1** was dramatically changed to intensive red in 16 h, and the red crystals were filtered off and washed briefly with DMF. The resultant solid, **1**⊃nitrobenzene, was characterized by IR, UV/vis, and fluorescence spectroscopies, elemental analysis, and XPS. FT-IR for **1**⊃nitrobenzene (Nujol mull): $\nu_{C=O(DMF)}$ 1674, $\nu_{O-C=O(carboxylate)}$ 1595, $\nu_{C=C(aromatic)}$ 1557, $\nu_{O-C=O(carboxylate)}$ and $\nu_{NO_2}$ 1532, 1347, $\nu_{C-N}$ 852 $cm^{-1}$. Anal. Calcd for $Li_4C_{54}H_{55}O_{18}N_7$: C, 58.02; H, 4.96; N, 8.77. Found: C, 59.01; H, 4.59; N, 8.70. Upon soaking **1** in nitrobenzene, two coordinated DMF molecules to Li4 are exchanged by two water molecules, which is evidenced by single-crystal XRD. One nitrobenzene molecule and two coordinating water molecules are crystallographically detected, and the other guest molecules in **1**⊃nitrobenzene are identified by elemental analysis, IR spectroscopy, and TGA.

**Powder XRD (PXRD) Analysis.** After compounds **1** and **1**⊃nitrobenzene were ground, the powder was filled in the capillary, respectively (diameter, 0.4 mm; wall thickness, 0.01 mm). Those diffraction data were collected at 95 K with 200 mm detector distance in 600 s exposure with synchrotron radiation ($\lambda$ = 0.79984 Å) on an ADSC Quantum-210 detector at 2D SMC with a silicon(111) double-crystal monochromator (DCM) at the Pohang Accelerator Laboratory, Korea. The *ADX* program[16] was used for data collection, and the *Fit2D* program[17] was used for conversion of a two-dimensional diffraction image to a one-dimensional diffraction pattern.

**Single-Crystal X-ray Crystallography.** Single crystals of **1** and **1**⊃nitrobenzene coated with paratone-*N* oil were mounted on the loop, and those diffraction data were collected at 95 K with synchrotron radiation ($\lambda$ = 0.74999 Å) on a ADSC Quantum-210 detector at 2D SMC with a silicon(111) DCM at the Pohang Accelerator Laboratory, Korea. The ADSC Q210 *ADX* program[16] was used for data collection, and *HKL2000* (version 699.18) for **1** and *HKL3000sm* (version 703r)[18] for **1**⊃nitrobenzene were used for cell refinement, reduction, and absorption correction.

The crystal structure of **1** was solved by the direct space method with the *SIR2011* program[19] and refined by full-matrix least-squares calculations with the *SHELX-TL* (version 2008) program package.[20] Two ligands, four Li ions, and two coordinated DMF molecules were observed as an asymmetric unit. Thermal factors of nitrogen (N1A) and carbon (C1A) atoms in a coordinated DMF molecule were restrained by using SIMU, DELU, and ISOR during the least-squares refinement. The crystal structure of **1**⊃nitrobenzene was solved by a direct method with the *SHELXTL-XS* program[20] and refined by full-matrix least-squares calculations with the *SHELX-TL* (version 2008) program package.[20] Two ligands, four Li ions, two coordinated water molecules, and one nitrobenzene molecule as a guest were observed as an asymmetric unit. After soaking **1** in nitrobenzene, its single crystallinity was decreased to result in inferior quality of the data to **1**. The nitro group in a nitrobenzene molecule was restrained using DFIX, DANG, SIMU, and DELU during the least-squares refinement. For both structures, all non-H atoms were refined anisotropically. The H atoms were assigned isotropic displacement coefficients $U$(H) = 1.2$U$(C,N) or 1.5$U(C_{methyl})$, and their coordinates were allowed to ride on their respective atoms. All of the methyl H atoms and some H atoms on the C atoms were not included during the least-squares refinement. Even though the electron densities of some guest solvent molecules were found, those could not be well modeled in the refinement because of severe disorder. The final refinement was performed with modification of the structure factors for contribution of the disordered solvent electron densities using the *SQUEEZE* option of *PLATON*.[21] The crystallographic data of **1** and **1**⊃nitrobenzene are summarized in Table 1. Further crystallographic details for the structure reported in this paper can be obtained from the Cambridge Crystallographic Data Center, on quoting the depository numbers CCDC 874240 for **1** and 874241 for **1**⊃nitrobenzene.

## RESULTS AND DISCUSSION

**Synthesis.** To construct a luminescent MOF, we designed an organic building block that can induce intraligand charge transfer (ILCT) through the coexistence of electron donor and acceptor groups in a molecule. Because the charges in $H_2$CPMA can be transferred from the *N*-methylamino donor group to an acceptor carboxylate group, $H_2$CPMA is a good candidate ligand for the construction of luminescent MOFs


dx.doi.org/10.1021/ic3011458 | *Inorg. Chem.* 2013, 52, 589−595

**Table 1. X-ray Crystallographic Data of 1 and 1⊃Nitrobenzene (*SQUEEZE* Data)**

| | 1 | 1⊃nitrobenzene |
|---|---|---|
| formula | $Li_4C_{36}H_{36}N_4O_{10}$ | $Li_4C_{36}H_{31}N_3O_{12}$ |
| cryst syst | orthorhombic | orthorhombic |
| space group | *Iba*2 | *Iba*2 |
| fw | 712.45 | 725.40 |
| *a*, Å | 28.467(6) | 28.710(6) |
| *b*, Å | 28.594(6) | 28.737(6) |
| *c*, Å | 12.960(3) | 12.883(3) |
| *V*, Å$^3$ | 10549(4) | 10629(4) |
| *Z* | 8 | 8 |
| $\rho_{calcd}$, g cm$^{-3}$ | 0.897 | 0.907 |
| temp, K | 95(2) | 95(2) |
| $\lambda$, Å | 0.74999 | 0.90000 |
| $\mu$, mm$^{-1}$ | 0.048 | 0.091 |
| GOF ($F^2$) | 1.070 | 2.042 |
| $F$(000) | 2976 | 3008 |
| reflns collected | 44991 | 23112 |
| indep reflns | 13000 [$R$(int) = 0.0423] | 7225 [$R$(int) = 0.0533] |
| completeness to $\theta_{max}$, % | 99.1 | 95.0 |
| data/param/restraints | 13000/491/20 | 7225/466/6 |
| $\theta$ range for data collection, deg | 2.13−30.00 | 2.54−30.00 |
| diffraction limits ($h$, $k$, $l$) | $-37 \le h \le 37$, $-37 \le k \le 37$, $-17 \le l \le 17$ | $-31 \le h \le 31$, $-28 \le k \le 29$, $-14 \le l \le 14$ |
| refinement method | full-matrix least squares on $F^2$ | full-matrix least squares on $F^2$ |
| R1, wR2 [$I > 2\sigma(I)$] | 0.0862,[a] 0.2447[b] | 0.1906,[a] 0.4563[c] |
| R1, wR2 (all data) | 0.0884,[a] 0.2489[b] | 0.2087,[a] 0.4817[c] |
| largest peak, hole, e Å$^{-3}$ | 0.477, −0.271 | 0.800, −0.645 |

[a] $R1 = \sum||F_o| - |F_c||/\sum|F_o|$. [b] $wR2(F^2) = [\sum w(F_o^2 - F_c^2)^2/\sum w(F_o^2)^2]^{1/2}$, where $w = 1/[\sigma^2(F_o^2) + (0.1940P)^2 + (1.73)P]$, $P = (F_o^2 + 2F_c^2)/3$. [c] $wR2(F^2) = [\sum w(F_o^2 - F_c^2)^2/\sum w(F_o^2)^2]^{1/2}$, where $w = 1/[\sigma^2(F_o^2) + (0.2000P)^2 + (0.0000)P]$, $P = (F_o^2 + 2F_c^2)/3$.

(Scheme 1). $H_2$CPMA was successfully prepared via the halogen−lithium exchange reaction of bis(4-bromophenyl)-*N*-

**Scheme 1. Schematic Structure of Organic Ligand $H_2$CPMA**

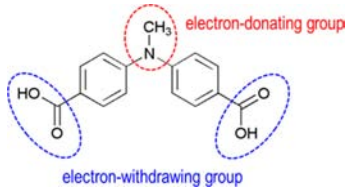


methylamine and subsequent carbonation of the resultant dilithio compound (Figure S1 in the Supporting Information). The solvothermal reaction of $Li(NO_3)\cdot 6H_2O$ with $H_2$CPMA in DMF as the solvent yielded pale-yellow crystals of **1**.

While transition metals are commonly used and those coordination geometries have been well-studied in MOFs, alkali- and alkaline-earth-metal ions were limitedly used to construct MOFs despite the advantages. Especially for application for hydrogen storage, because of the highly electropositive nature of a Li ion, it is expected to induce strong electrostatic interaction with hydrogen molecules in MOFs.[22] In addition, Li-based MOFs ensure a gravimetric advantage because of the lightest weight of Li among metals. The introduction of Li ions into MOFs could be achieved by doping Li ions on the surface or in the pores of MOFs.[23] However, direct uses of Li salt as a metal building block to synthesize three-dimensional MOFs are still rare.[24,25] Parise et al. reported several kinds of three-dimensional Li-MOFs designated as ULMOFs (UL = ultralight), which were constructed by the solvothermal syntheses of Li cation and carboxylate ligands such as 4,4′-biphenyldicarboxylate ($BPDC^{2-}$), napthalenedicarboxylate (2,6-$NDC^{2-}$), sulfonyldibenzoate ($SDB^{2-}$), 2,5-pyridinedicarboxylate (2,5-$PDC^{2-}$), 2,6-pyridinedicarboxylate (2,6-$PDC^{2-}$), and 3,5-pyridinedicarboxylate (3,5-$PDC^{2-}$).[24] The Li-MOFs showed interesting properties of the dynamic structural behavior[24b] and exceptionally high thermal stability.[24c] Robson et al. successfully synthesized a lithium isonicotinate framework, which showed the high heat of adsorption value of 9.9 kJ mol$^{-1}$ for hydrogen gas, and the results provided proof of concept for hydrogen storage materials.[25a]

**Crystal Structure.** The structure of **1**, which was determined by single-crystal XRD (Table 1), consisted of Li−O chains as the secondary building units (SBUs) and bridging ligands (Figures 1a and S2 in the Supporting Information). Compound **1** possesses four crystallographically independent Li atoms in distorted tetrahedral coordination geometry, for which the bond lengths and angles are listed in Table S1 in the Supporting Information.

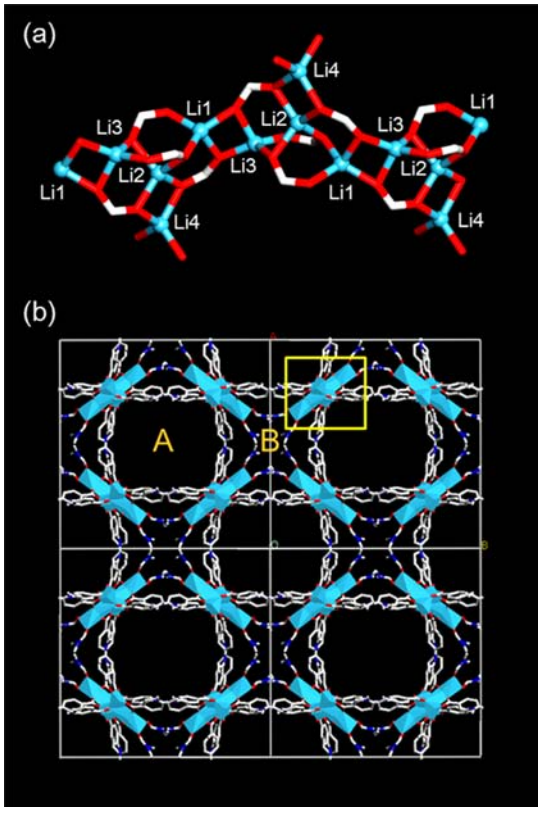


**Figure 1.** Single-crystal X-ray structure of **1**. (a) SBU of the Li−O chain. (b) Three-dimensional framework formed by the association of SBUs and organic ligands, projected along the *c* axis. H atoms and noncoordinating guest molecules are omitted for clarity. Color scheme: C, white; O, red; N, blue; Li, light blue. The yellow rectangle indicates the SBU of the Li−O chain.


dx.doi.org/10.1021/ic3011458 | *Inorg. Chem.* 2013, 52, 589−595

As shown in Figure 1a, Li1, Li2, and Li3 are bonded by four carboxylate O atoms, associated with four different $CPMA^{2-}$ moieties (bond lengths of Li−O: 1.910−2.016 Å). Li4 also has a tetrahedral geometry and is coordinated with two O atoms from two different carboxylate groups [Li−O, av. 1.994(5) Å] and two carbonyl O atoms of DMF [Li−O, av. 1.911(6) Å]. The tetrahedrally coordinated Li ions generate one-dimensional Li−O chains as SBUs, which are bridged with four neighboring chains by dicarboxylate ligands, $CPMA^{2-}$, in four different directions (Figure 1b). As a result, a three-dimensional $\{Li_3[Li(DMF)_2](CPMA)_2\}_n$ network is constructed with two kinds of rectangular channels, A and B, along the *c* axis. Channel A, of 13.4 × 10.4 Å, is occupied by free guest molecules, DMF and water, and channel B of 12.3 × 9.5 $Å^2$ is filled with Li4-coordinating DMF molecules. In Figure 2a and

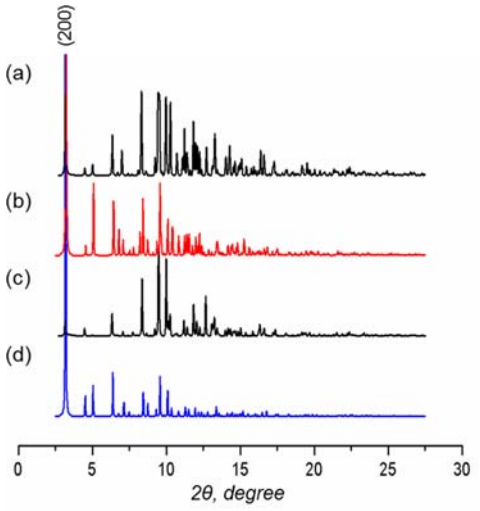


**Figure 2.** Synchrotron PXRD data ($\lambda$ = 0.79984 Å) measured at 95 K for (a) as-synthesized **1** and (c) **1**⊃nitrobenzene and simulated patterns from single-crystal XRD data of (b) as-synthesized **1** and (d) **1**⊃nitrobenzene.

b, the PXRD pattern of the as-synthesized **1** is compared with the simulated pattern based on the single-crystal XRD data. It shows a slight change in the peak positions and relative intensity from those in the calculated pattern. This might be attributed to the dynamic behavior of **1** upon the existence of guest molecules, which is affected by the sample preparation procedure. However, the space group extracted from the measured pattern appeared to be the same as that of the single-crystal XRD data (Figure S3 in the Supporting Information). This means that the bulk and single crystal are the same materials, and the only differences of the XRD patterns unavoidably happened because of the nature of the materials.

**Framework Stability.** In the TGA trace of as-synthesized **1** (Figure S4 in the Supporting Information), the guest solvent molecules occupied in channel A of **1** can be removed in the range from room temperature to ca. 160 °C with an experimentally determined weight loss of 31.2%, which shows a good agreement with the calculated one of 30.3%. To remove coordinating DMF molecules from Li4, the temperature should reach around 450 °C, followed by decomposition of **1**. *PLATON* calculations indicate that **1** contains 40.3% void space (4276.5 $Å^3$ per unit cell volume) for accessing the guest molecules per unit cell. The gas-sorption isotherm for dried Li-MOF **1** showed no porosity, as shown in the $N_2$-sorption isotherm (Figure S5 in the Supporting Information), because Li-MOF **1** showed the flexible behavior according to the existence of guest molecules, as evidenced by PXRD in Figure S6 in the Supporting Information. The disappearance of the (200) peak at the range of low angles exhibits the collapse of channels in Li-MOF, resulting in a structure different from that of the as-synthesized compound.

**Detection Studies.** To see the specific analyte detection ability of **1**, compound **1** is soaked in nitrobenzene, 2,4-dinitrotoluene (DNT), benzene, and toluene. Because DNT is a solid phase at room temperature, **1** is immersed in a concentrated DMF solution of DNT, and other solvents are used as neat. When Li-MOF **1** is immersed in nitrobenzene and DNT, it shows a dramatic color change from pale yellow to red and deep orange, respectively. In contrast, **1** remains its original color upon soaking in benzene and toluene (Figure S7 in the Supporting Information). Thus, **1** has the ability to detect nitroaromatic compounds selectively, and **1** containing nitrobenzene molecules is scrutinized to understand the sensing mechanism. Li-MOF **1** absorbs three nitrobenzene molecules per formula unit, yielding **1**⊃nitrobenzene, as evdenced by elemental analysis. In Figure 3, a comparison of the IR spectra

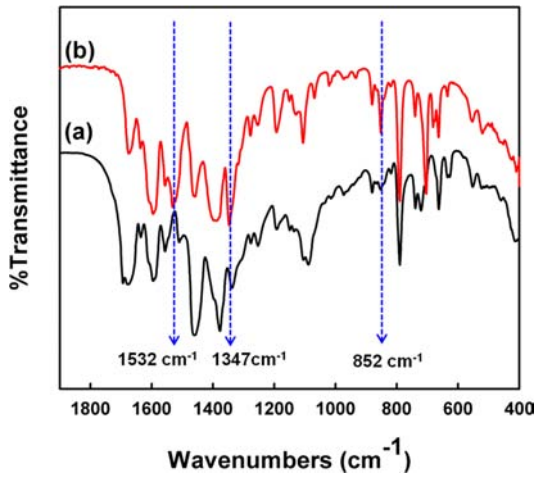


**Figure 3.** Transmission FT-IR spectra of (a) **1** (black) and (b) **1**⊃nitrobenzene (red). The FT-IR spectrum of **1**⊃nitrobenzene clearly shows an asymmetric $NO_2$ stretch (1532 $cm^{-1}$), a symmetric $NO_2$ stretch (1347 $cm^{-1}$), and a C−N stretch for $ArNO_2$ (852 $cm^{-1}$).

of **1** and **1**⊃nitrobenzene shows that **1**⊃nitrobenzene has additional peaks at 1532 [$\nu_a(NO_2)$], 1347 [$\nu_s(NO_2)$], and 852 [$\nu_s(C-N)$] $cm^{-1}$, which correspond with the typical peaks of nitrobenzene. The XPS results also clearly show the inclusion of nitrobenzene in **1** (Figure S8 in the Supporting Information). The UV/vis absorption spectrum of **1** in the solid state (Figure S9 in the Supporting Information) shows two absorption peaks, at 248 and 352 nm, which means that there is no significant color in the visible region. However, when the as-synthesized **1** absorbs nitrobenzene, the obtained **1**⊃nitrobenzene exhibits a deep-red color (Figure 4a); this is proven spectroscopically by the appearance of an additional absorption peak at around 500 nm (Figure S9 in the Supporting Information). The intense red color of **1**⊃nitrobenzene is attributed to the charge-transfer transition between the aromatic rings of the electron-rich $CPMA^{2-}$ molecules and the electron-deficient nitrobenzene due to the strong electron-withdrawing $-NO_2$ group. **1** is reversibly regenerated in 5 min


dx.doi.org/10.1021/ic3011458 | *Inorg. Chem.* 2013, 52, 589−595

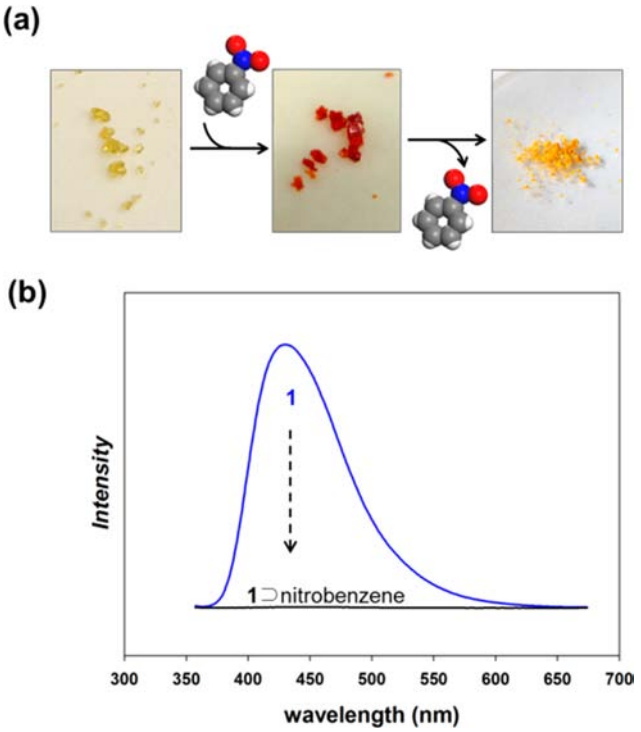


**Figure 4.** Detection of nitrobenzene in **1**. (a) Photographs of **1**, **1**⊃nitrobenzene, and **1** regenerated by heating. (b) Fluorescence spectra of **1** and **1**⊃nitrobenzene.

simply by heating the nitrobenzene-absorbed **1** at 100 °C under vacuum, as is readily observed by the color change. Such visualization of the uptake of harmful molecules in the solid state provides great opportunities for utilizing this MOF as a sensor.

The other approach for sensing nitroaromatic explosives is fluorescence quenching upon detection. Because our aim was to generate fluorophores in a MOF by using a tailored organic ligand as a building block, the emission spectrum of **1** was recorded in the solid state. The MOF **1** exhibits an intense emission at $\lambda_{max}$ = 430 nm when it is excited at 345 nm. The emission in **1** is derived from a strong ILCT from the donor *N*-methylamino group to the acceptor carboxylate groups in the $CPMA^{2-}$ molecule. On the contrary, **1**⊃nitrobenzene is completely nonemissive under excitation at 345 nm (Figure 4b). The same response occurs in **1**⊃DNT, as shown in Figure S10 in the Supporting Information. This fluorescence-quenching phenomenon can be explained by an electron-transfer donor–acceptor mechanism via host–guest interactions.[5,26] To see the detection behavior of **1** upon concentration of explosive materials, the fluorescence spectra for MOF **1** after immersion in various concentration solutions of nitrobenzene/DMF were obtained (Figure S11 in the Supporting Information). Upon increasing concentration of nitrobenzene in DMF ($2.4 \times 10^{-2}$ M ~ neat nitrobenzene), the maximum intensity of the fluorescence spectrum was decreased. To clearly show the relative intensities, the percentage of fluorescence was plotted in Figure S11b in the Supporting Information, which was estimated using the formula $(I_a/I_0) \times 100\%$, where $I_0$ is the maximum intensity of Li-MOF **1** and $I_a$ is the maximum intensity of Li-MOF **1** after immersion in an *a* M nitrobenzene/DMF solution. From its fitting curve, the concentration for half-quenching of the fluorescence is calculated as 0.048 M of a nitrobenzene/DMF solution.

**Single-Crystal-to-Single-Crystal Transformation.** When **1** is immersed in nitrobenzene, the molecules are easily included as guests in the channels of **1**, for which the driving forces are these effective interactions of nitrobenzene with the inner surface of **1**. As shown in Figure 4a, even after the absorption of nitrobenzene, **1** preserves its single-crystalline nature. Therefore, the host–guest interaction in **1**⊃nitrobenzene is observed directly by single-crystal XRD, and this accounts for the luminescence quenching as well as the crystal color change. In Figure 2c and d, the PXRD pattern of **1**⊃nitrobenzene is coincident with the simulated pattern based on the single-crystal XRD data, showing the homogeneous uptakes of nitrobenzene in **1**. The X-ray structures of **1** and **1**⊃nitrobenzene are clearly compared in Figure 5. The confined nitrobenzene molecules in the channels of **1** lead to strong $\pi-\pi$ stacking with three benzene rings belonging to two neighboring $CPMA^{2-}$ units in the framework (shortest C···C distances = 3.455, 3.550, and 3.849 Å, respectively; Figure 5a). Furthermore, strong interaction between the nitro group and the benzene ring of a $CPMA^{2-}$ ligand is revealed by a short

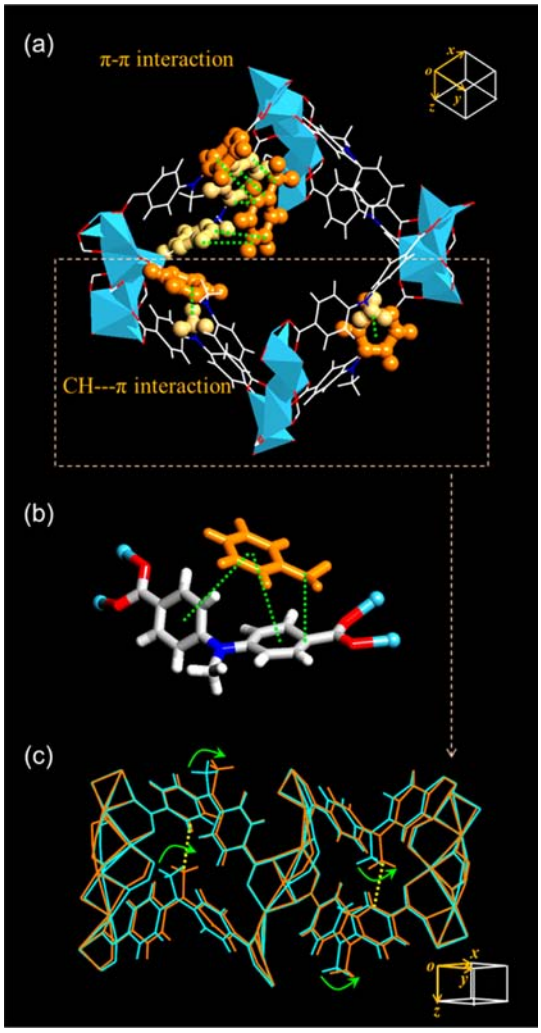


**Figure 5.** (a) X-ray structure of **1**⊃nitrobenzene, in which $\pi-\pi$ and C–H···$\pi$ interactions are emphasized by the orange ball-and-stick representation (color scheme: C, white; O, red; N, blue; Li, light blue). (b) Close-up shot of the interaction between nitrobenzene (orange) and $CPMA^{2-}$ incorporated in **1**. (c) Comparison of the superimposed X-ray structures of **1** (cyan) and **1**⊃nitrobenzene (orange).


dx.doi.org/10.1021/ic3011458 | *Inorg. Chem.* 2013, 52, 589–595

distance of $N_{nitro}\cdots C_{CPMA^{2-}}$ of 3.091 Å. A close-up shot of the interaction between nitrobenzene and one of $CPMA^{2-}$ ligands incorporated in **1** is shown in Figure 5b. In this range of interactions, the electron-deficient nitrobenzene can act as an electron acceptor for the photoexcited electrons of **1**, resulting in electron transfer from the MOF to nitrobenzene, followed by back electron transfer instead of fluorescence. Moreover, as shown in the superimposed X-ray structures of **1** and **1**⊃nitrobenzene (Figure 5c), $\pi-\pi$ interactions cause the molecular dynamics of the flexible ligand $CPMA^{2-}$; meanwhile, the methyl group of $CPMA^{2-}$ approaches the neighboring benzene ring of $CPMA^{2-}$ to induce C−H$\cdots\pi$ interactions in the framework. The $C_{methyl}\cdots$centroid distances decrease from 4.359 to 4.050 Å after nitrobenzene inclusion. This interligand interaction also contributes to the change in the electronic structure of **1**, quenching the fluorescence.

## CONCLUSIONS

In conclusion, we introduced a well-defined ditopic organic ligand, $H_2$CPMA, for the potential provision of the luminescence properties in MOFs and the successful preparation of the luminescent three-dimensional Li-based MOF. A luminescent Li-based MOF detected explosive nitroaromatic compounds selectively by showing an intensive color change as well as luminescence quenching in the solid state. We provided direct evidence for interaction sites in the MOF toward the nitroaromatic compound via single-crystal XRD of MOF containing nitroaromatic compounds. Strong interaction between the MOF and included compounds explained the alteration of the electronic structure of the MOF. This result will afford in-depth understanding to help in the design of MOFs as sensors, in which the specific sites to interact with analytes are introduced.

## ASSOCIATED CONTENT

### Supporting Information

X-ray crystallographic files in CIF format, X-ray crystallographic table, ORTEP drawing of **1**, TGA trace of **1**, XRD patterns of Li-MOF **1** and dried MOF, gas-sorption isotherms of Li-MOF **1**, photographs of **1** after immersion in various solvents, N 1s XPS result of **1**⊃nitrobenzene, UV/vis spectra of **1** and **1**⊃nitrobenzene, fluorescence spectra of **1**⊃DNT, and concentration-dependent fluorescence spectra. This material is available free of charge via the Internet at http://pubs.acs.org.

## AUTHOR INFORMATION

### Corresponding Author

*E-mail: dmoon@postech.ac.kr (D.M.), hoirimoon@unist.ac.kr (H.R.M.). Tel: +82-52-217-2928. Fax: +82-52-217-2019.

### Notes

The authors declare no competing financial interest.

## ACKNOWLEDGMENTS

This work was supported by Basic Science Research Program through the National Research Foundation of Korea funded by the Ministry of Education, Science and Technology (Grants 2011-0004358 and 2012-002507). X-ray crystallography at the PLS-II 2D SMC beamline was supported, in part, by MEST and POSTECH.

## REFERENCES

(1) (a) Kaye, S. S.; Dailly, A.; Yaghi, O. M.; Long, J. R. *J. Am. Chem. Soc.* **2007**, *129*, 14176−14177. (b) Lee, Y.-G.; Moon, H. R.; Cheon, Y. E.; Suh, M. P. *Angew. Chem., Int. Ed.* **2009**, *47*, 7741−7745.

(2) (a) Corma, A.; Garcia, H.; Xamena, F. X. L. I *Chem. Rev.* **2010**, *110*, 4606−4655. (b) Ishida, T.; Nagaoka, M.; Akita, T.; Haruta, M. *Chem.—Eur. J.* **2008**, *14*, 8456−8460. (c) El-Shall, M. A.; Abdelsayed, V.; Khder, A. E. R. S.; Hassan, H. M. A.; El-Kaderi, H. M.; Reich, T. E. *J. Mater. Chem.* **2009**, *19*, 7625−7631.

(3) (a) Bureekaew, S.; Sato, H.; Matsuda, R.; Kubota, Y.; Hirose, R.; Kim, J.; Kato, K.; Takata, M.; Kitagawa, S. *Angew. Chem., Int. Ed.* **2010**, *49*, 7660−7664. (b) Henke, S.; Fischer, R. A. *J. Am. Chem. Soc.* **2011**, *133*, 2064−2067.

(4) Lan, A. J.; Li, K. H.; Wu, H. H.; Olson, D. H.; Emge, T. J.; Ki, W.; Hong, M.; Li, J. *Angew. Chem., Int. Ed.* **2009**, *48*, 2334−2338.

(5) Pramanik, S.; Zheng, C.; Zhang, X.; Emge, T. J.; Li, J. *J. Am. Chem. Soc.* **2011**, *133*, 4153−4155.

(6) Xu, H.; Liu, F.; Cui, Y.; Chen, B.; Qian, G. *Chem. Commun.* **2011**, *47*, 3153−3155.

(7) Zhang, Z.; Xiang, S.; Rao, X.; Zheng, Q.; Fronczek, F. R.; Qian, G.; Chen, B. *Chem. Commun.* **2010**, *46*, 7205−7207.

(8) Liu, J.; Sun, F.; Zhang, F.; Wang, Z.; Zhang, R.; Wang, C.; Qiu, S. *J. Mater. Chem.* **2011**, *21*, 3775−3778.

(9) Zhao, D.; Timmons, D. J.; Yuan, D.; Zhou, H.-C. *Acc. Chem. Res.* **2011**, *44*, 123−133.

(10) Yaghi, O. M.; O'Keeffe, M.; Ockwig, N. W.; Chae, H. K.; Eddaoudi, M.; Kim, J. *Nature* **2003**, *423*, 705−714.

(11) Wang, R.; Zhang, J.; Li, L. *Inorg. Chem.* **2009**, *48*, 7194−7200.

(12) Kuc, A.; Enyashin, A.; Seifert, G. *J. Phys. Chem. B* **2007**, *111*, 8179−8186.

(13) Cao, W.; Li, Y.; Wang, L.; Liao, S. *J. Phys. Chem. C* **2011**, *115*, 13829−13836.

(14) (a) Bauer, C. A.; Timofeeva, T. V.; Settersten, T. B.; Patterson, B. D.; Liu, V. H.; Simmons, B. A.; Allendorf, M. D. *J. Am. Chem. Soc.* **2007**, *129*, 7136−7144. (b) Cui, Y.; Yue, Y.; Qian, G.; Chen, B. *Chem. Rev.* **2012**, *112*, 1126−1162. (c) Allendorf, M. D.; Bauer, C. A.; Bhakta, R. K.; Houk, R. J. *Chem. Soc. Rev.* **2009**, *38*, 1330−1352.

(15) Laliberte, B. R.; Leone, S. A. *J. Organomet. Chem.* **1972**, *37*, 209−215.

(16) Arvai, A. J.; Nielsen, C. *ADSC Quantum-210 ADX Program*; Area Detector System Corp.; Poway, CA, 1983.

(17) *Fit2D* program: Andy Hammersley (e-mail: hammersley@esrf.fr), ESRF, 6 rue Jules Horowitz, BP 220, 38043 Grenoble Cedex 9, France.

(18) Otwinowski, Z.; Minor,W. In *Methods in Enzymology*; Carter, C. W., Jr., Sweet, R. M., Eds.; Academic Press: New York, 1997; Vol. *276*, Part A, p 307.

(19) Burla, M. C.; Caliandro, R.; Camalli, M.; Carrozzini, B.; Cascarano, G. L.; Giacovazzo, C.; Mallamo, M.; Mazzone, A.; Polidori, G.; Spagna, R. *J. Appl. Crystallogr.* **2012**, *45*, 357−361.

(20) Sheldrick, G. M. *SHELXTL-PLUS, Crystal Structure Analysis Package*; Bruker Analytical X-ray: Madison, WI, 1997.

(21) *PLATON* program: Spek, A. L. *Acta Crystallogr., Sect. A* **1990**, *46*, 194−201.

(22) Rao, D.; Lu, T.; Xiao, C.; Kan, E.; Deng, K. *Chem. Commun.* **2011**, *47*, 7698−7700.

(23) Mulfort, K. L.; Hupp, J. T. *J. Am. Chem. Soc.* **2007**, *129*, 9604−9605.

(24) (a) Banerjee, D.; Borkowski, L. A.; Kim, S. J.; Parise, J. B. *Cryst. Growth Des.* **2009**, *9*, 4922−4926. (b) Banerjee, D.; Kim, S. J.; Li, W.; Wu, H.; Li, J.; Borkowski, L. A.; Philips, B. L.; Paries, J. B. *Cryst. Growth Des.* **2010**, *10*, 2801−2805. (c) Banerjee, D.; Kim, S. J.; Paries, J. B. *Cryst. Growth Des.* **2009**, *9*, 2500−2503. (d) Banerjee, D.; Kim, S. J.; Borkowski, L. A.; Xu, W.; Paries, J. B. *Cryst. Growth Des.* **2010**, *10*, 709−715.

(25) (a) Abrahams, B. F.; Grannas, M. J.; Hudson, T. A.; Robson, R. *Angew. Chem., Int. Ed.* **2010**, *49*, 1087−14089. (b) Liu, Y.-Y.; Zhang, J.; Xu, F.; Sun, L.-X.; Zhang, T.; You, W.-S.; Zhao, Y.; Zeng, J.; Cao, Z.; Yang, D. *Cryst. Growth Des.* **2008**, *8*, 3127−3129.

(26) Toal, S. J.; Trogler, W. C. *J. Mater. Chem.* **2006**, *16*, 2871−2883.



dx.doi.org/10.1021/ic3011458 | *Inorg. Chem.* 2013, 52, 589−595